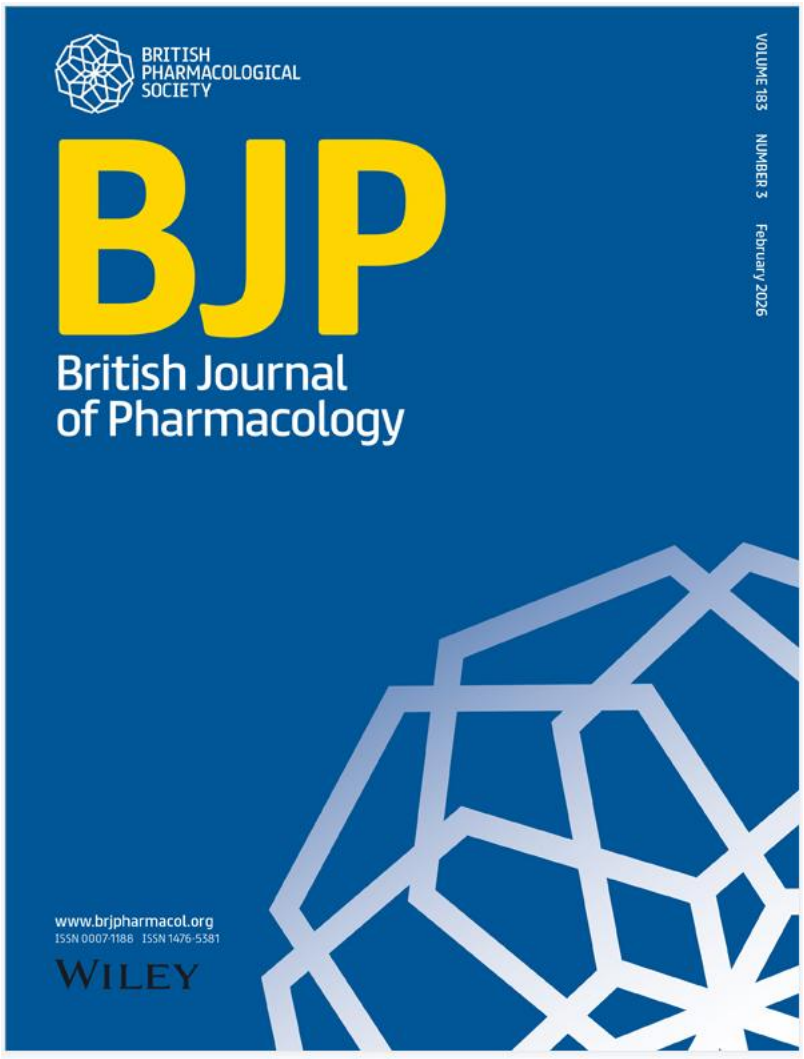
BRITISH
PHARMACOLOGICAL
SOCIETY
BJP
British Journal
of Pharmacology
VOLUME 183 NUMBER 3 February 2026
www.brjpharmacol.org
ISSN 0007-1188 ISSN 1476-5381
WILEY

compared to the situation in tissues from control animals. CS014 induced a robust, dose-dependent amelioration of the vascular remodelling induced by the Sugen/hypoxia protocol with reduced arteriolar vessel occlusion, intimal proliferation (including a reduction of plexiform lesions) and fibrosis. The efficacy or maximum effect of CS014 on the global arterial score (GAS), which reflects the extent of vascular occlusion, corresponded to a 50% reduction in values seen in the vehicle controls (shown in the figure). This occurred at estimated areas under the 24-h plasma CS014-FA curve (AUC) > 250 h.µg/ml corresponding to unbound AUCs >68 µg/ml.h. The estimated AUC required to achieve 50% of the efficacy was 122 h.µg/ml, corresponding to an unbound AUC of 33.3 µg/ml.h. There was a tendency for CS014 to lower the RV weight; however, this effect was not dose-dependent and was only statistically significant in the 40 mg/kg dose group compared to the Vehicle Controls.

Conclusion

CS014 treatment for 3 weeks decreased perivascular fibrosis and dose-dependently ameliorated pulmonary arteriolar vascular remodelling, including reduction in plexiform lesions, in the Sugen/hypoxia rat model of PAH.

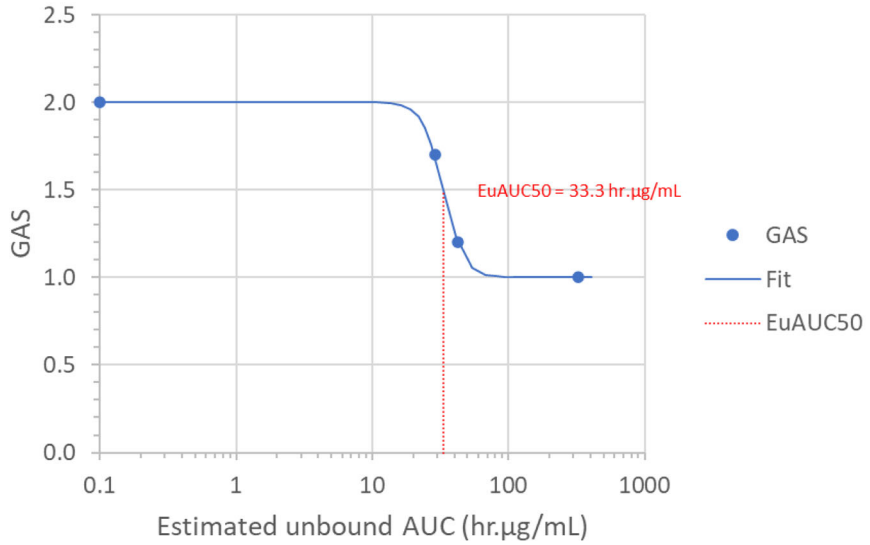

Mean GAS values for the 4 groups of Sugen/hypoxia animals (vehicle control and 3 groups of CS014 treated animals, 20, 40 and 300 mg/kg, n=7-10/group) are plotted against corresponding estimated unbound CS014 AUCs (blue circles). A logistic function curve fit (blue line) was used to estimate the effective unbound AUC at which 50% of the maximal CS014 effect was reached ($EuAUC_{50}$). Note that the AUC for the vehicle control group is arbitrarily set at a low level of 0.1 hr.µg/mL to allow visualization on the logarithmic scale.

260 | Comparison of the effects of niacin and a germanium–niacin complex on the fatty acid content of the brain, heart, liver and kidneys in female rats with acute ethanol intoxication

Iryna Nizhenkovska, Violetta Narokha, Olena Kuznetsova
Bogomolets National Medical University

Introduction

According to WHO data, the morbidity and mortality associated with alcohol use disorders remain high despite a decline in overall consumption levels. Ethanol intoxication, both acute and chronic, has a profound impact on cellular components, the functional alterations of which may lead to cell necrosis not only in the liver but also in other organs such as the brain, heart and kidneys. Niacin is an essential human nutrient and has the ability to influence lipid metabolism. There is evidence that the complexation of organic molecules with metals may enhance their activity and provide new pharmacological effects. In particular, coordination compounds of germanium with niacin have demonstrated protective properties under conditions of toxic damage of various origins.

Method

The study was conducted on female Wistar rats, which were divided into five groups of seven animals each (n = 7). The animals were maintained in accordance with the requirements of EU Directive 2010/63/EU. Acute intoxication was induced by a single administration of 50% ethanol at a dose of 5 ml/kg b.w. via gastric gavage (group 2). Rats in the control group received distilled water instead of ethanol (group 1). Niacin (at a dose of 100 mg/kg b.w., aqueous solution; group 3) and the coordination compound of germanium (VI) with niacin [1] with laboratory code MIGU-1 (at doses of 100 mg/kg and 65 mg/kg b.w., aqueous solution; groups 4 and 5, respectively) were administered once intraperitoneally 1 h prior to ethanol intoxication. Organs were collected 1 h after administration of ethanol. The qualitative composition and quantitative content of fatty acids

(FAs) in the brain, heart, liver and kidney tissues were analysed by gas chromatography. Nine FAs were identified: C14:0, C15:0, C16:0, C17:0 and C18:0 (which comprised the total saturated fatty acids [∑SFA]) and C18:1, C18:2, C18:3 and C20:4 (which comprised the total unsaturated fatty acids [∑UFA]). The total polyunsaturated fatty acids (∑PUFA) included C18:2, C18:3 and C20:4.

Results

Ethanol administration was associated with an alteration in the fatty acid profile, manifested by a decrease in SFAs in the brain and their increase in other organs. In the brain, the ∑USFA increased by 22%. In the heart, overall, there was a significant 21% increase in ∑SFA. In the liver, ∑PUFA levels significantly decreased due to reductions in C18:2 and C20:4. In the kidneys, ∑PUFA levels decreased, accompanied by an 18% increase in ∑SFA.

Following niacin administration, the ∑SFA/∑USFA ratio in the brain and heart was restored to control values, whereas in the liver and kidneys the ∑SFA level remained elevated by 30% and 18%, respectively.

After administration of MIGU-1 at a dose of 100 mg/kg, normalization of C16:0, C18:0 and C18:1 levels to control values was observed in the brain, along with a decrease in ∑PUFA levels due to reductions in C18:2 and C20:4. In the heart, normalization of C16:0 to the control level was noted, accompanied by an increase in C18:0 and a decrease in C18:1. A 10% change in ∑PUFA levels was characterized by a reduction in C18:2 and an increase in C20:4. In the liver, C16:0 and C18:0 increased, while C18:1 remained unchanged. A marked 81% decrease in ∑PUFA levels was observed, due to reductions in C18:2 and C20:4. In the kidneys, a decrease in C16:0 and an increase in C18:0 and C18:1 were observed. ∑PUFA levels remained reduced by 24% due to an 80% decrease in C18:2, accompanied by a 17% increase in C20:4. Thus, after administration of MIGU-1 at a dose of 100 mg/kg, the ∑SFA/∑USFA ratio in the brain and kidneys was restored to control values, whereas in the heart and liver, ∑SFA levels remained elevated by 13% and 33%, respectively. Administration of MIGU-1 at a dose of 65 mg/kg resulted in restoration of the ∑SFA/∑USFA ratio to control values in the brain and liver, while in the heart and kidneys, it decreased by 24% and 10%, respectively.

Conclusions

Administration of niacin and the germanium–niacin complex normalized the fatty acid content in the brain, heart, liver and kidneys during acute ethanol intoxication; however, their efficacy depended on both the dose and the target organ. Further studies at different doses and elucidation of the biochemical mechanisms are required to confirm the therapeutic efficacy of this novel compound.

Reference

1. Seifullina II, Martsinko EE, Khristova NM, Chebanenko EA. Molecular complexes of germanium tetrachloride with niacin, nicotinic amide, isonicotinic hydrazide and their pharmacological actions. Visn Odes Nac Univ Him 2016; 21(2):18–28.

262 | Identifying brain-permeable CRAC channel inhibitors targeting CNS disorders

Aida Ashrafzadeh, Marcos Rubio Alarcon, Graham Ladds, Taufiq Rahman

Department of Pharmacology, University of Cambridge

Introduction

Store-operated calcium entry (SOCE), mediated by calcium release-activated calcium (CRAC) channels, is triggered by endoplasmic reticulum (ER) calcium depletion and is a key regulator of intracellular calcium dynamics [1]. Beyond replenishing ER stores, CRAC-mediated calcium signals activate the downstream nuclear factor of activated T-cell (NFAT) pathway, which controls gene expression programmes critical for immune and neuronal function.

CRAC channels are established targets, and small-molecule inhibitors have been developed to modulate their activity in peripheral inflammatory and autoimmune diseases. CRAC up-regulation has also been linked to CNS disorders, including autoimmune encephalomyelitis, neurodegeneration, neuropathic pain and brain cancers [2]. Nonetheless, development of brain-permeable inhibitors remains limited. This study aims to identify and characterize brain-penetrant SOCE inhibitors using an integrated computational and experimental approach.

Methods

A ligand-based virtual screen of 731 brain-permeable compounds was performed using ROCS and EON (OpenEye Scientific Software) to assess 3D shape and electrostatic similarity. Hits were ranked by shape, colour and 2D Tanimoto scores and the 20 top compounds were selected for validation (Figure 1).

Compounds were tested in Jurkat T cells using a FlexStation-based Ca^2 assay. Cells were plated on poly-D-lysine–coated 96-well plates, loaded with 2 μM Calbryte 520 AM and pre-incubated with DMSO, Pyr6 (3 μM) or test compounds for 30 min. SOCE was activated with 2 μM thapsigargin (Tg) and 600 μM extracellular Ca^2. Peak Ca^2 entry ([Ca^2]) was measured and normalized as $(F - Fmin)/(Fmax - F) \times Kd$. Experiments included ≥3 biological replicates.

NFAT signalling was assessed in Jurkat-Lucia™ NFAT-CD28 reporter cells. Compounds were pre-incubated for 30 min, and NFAT activation was induced by TCR (anti-CD3/CD28 Abs) or Tg stimulation. Luciferase activity was measured after 6 h. Cell viability was confirmed throughout.